Transformation mechanisms from metallic Zn nanocrystals to insulating $ZnSiO_3$ nanocrystals in a SiO_2 matrix due to thermal treatment

J. M. Yuk,[1] J. Y. Lee,[1] Y. S. No,[2] T. W. Kim,[2,a)] and W. K. Choi[3]
[1]*Department of Materials Science and Engineering, Korea Advanced Institute of Science and Technology, Daejeon 305-701, Republic of Korea*
[2]*Advanced Semiconductor Research Center, Electronics and Computer Engineering, Hanyang University, 17 Haengdang-dong, Seongdong-gu, Seoul 133-791, Republic of Korea*
[3]*Thin Film Materials Research Center, Korea Institute of Science and Technology, Seoul 136-791, Republic of Korea*

(Received 5 August 2008; accepted 12 November 2008; published online 3 December 2008)

Transmission electron microscopy (TEM), high-resolution TEM, and x-ray energy dispersive spectroscopy results showed that Zn metallic nanocrystals and $ZnSiO_3$ insulating nanocrytals embedded in a SiO_2 matrix were created from the ZnO thin films deposited on *n*-Si (001) substrates due to rapid thermal annealing. The formed Zn metallic nanocrystals were transformed into monoclinic $ZnSiO_3$ insulating nanocrystals with increasing number of Zn atoms resulting from an increase in the annealing time up to 10 min. The transformation mechanisms from metallic Zn nanocrystals to insulating $ZnSiO_3$ nanocrystals in a SiO_2 matrix due to rapid thermal annealing are described on the basis of the experimental results. © *2008 American Institute of Physics*.
[DOI: 10.1063/1.3040320]

Rapid advancements in nanocomposite-formation technologies have made possible the fabrication of various types of nanocomposites.[1] Among these nanocomposites, various nanocrystals embedded in an insulating matrix attract significant attention due to their promising applications in nonvolatile memory devices with low-power consumption and ultrahigh-density capability.[2–4] Various nanocrystals, such as metal,[5–7] semiconductor,[8–10] and insulating materials,[11] have been formed by using several techniques, such as ion implantation,[5] electron-beam-assisted oxidation,[6,8] rapid thermal annealing,[9–11] and selective chemical reaction.[7] Among these various methods for the formation of nanocrystals, the rapid thermal annealing is relatively simple and allows easier precise control of the size and the density of the nanocrystals without material damage in comparison with the other methods.[11] Even though some studies concerning the formation of nanocrystals, acting as charge-trapping islands, embedded in an insulating layer have been conducted,[3,4] studies concerning the transformation mechanisms from metallic Zn nanocrystals to insulating $ZnSiO_3$ nanocrystals embedded in an insulating matrix have not been performed yet.

This letter reports data on the mechanisms underlying the transformation from metallic Zn nanocrystals to insulating $ZnSiO_3$ nanocrystals embedded in SiO_2 layers in ZnO/*n*-Si heterostructures, formed by using plasma-assisted molecular beam epitaxy (PA-MBE) and thermal annealing. Transmission electron microscopy (TEM) and high-resolution TEM (HRTEM) measurements, together with fast-Fourier-transformed (FFT) electron-diffraction pattern simulations, were carried out to investigate the microstructural properties of the samples and to identify the existence of nanocrystals embedded in the ZnO/Si heterostructure. Energy dispersive x-ray spectroscopy (EDX) measurements were performed to characterize the stoichiometry of the heterointerface.

The carrier concentration of the P-doped *n*-Si substrates with (001) orientations used in this experiment was 1×10^{15} cm^{-3}. The substrates were degreased in trichloroethylene (TCE), rinsed in de-ionized water, etched in a mixture of HF and H_2O (1:1) at room temperature for 5 min, and rinsed in TCE again. The chemically cleaned Si wafers were mounted onto a molybdenum susceptor in a growth chamber for the spin glass assisted PA-MBE. The detailed growth procedure for the ZnO thin film is described elsewhere.[12] The thermal annealing process was performed in a nitrogen atmosphere with a tungsten-halogen lamp as the thermal source. The thermal annealing process was carried out for 5 or 10 min at 900 °C. The TEM measurements were performed by using a JEOL JEM 2100F transmission electron microscope operating at 200 kV. The resolution of the EDX attached to the Tecnai G2 F30 S-TWIN operating at 300 kV is 0.20 nm.

Figure 1 shows the cross-sectional bright-field TEM images of (a) the as-grown ZnO thin film grown on a *n*-Si (001) substrate and of (b) the ZnO thin film grown on a *n*-Si (001) substrate annealed at 900 °C for 5 min. An amorphous SiO_2 thin layer with a thickness of approximately 1 nm was naturally formed at an as-grown ZnO/*n*-Si (001) heterointerface.[11] When the as-grown sample was annealed at 900 °C for 5 min, an amorphous SiO_2 layer with a thickness of approximately 10 nm was formed between the ZnO thin film and the Si substrate, and one layer of metallic Zn nanocrystals with an average diameter of 5 nm was formed in the SiO_2 layer, as shown in Fig. 1(c). Figure 1(d) shows the EDX spectrum, taken from the circled area shown in Fig. 1(b), used to identify and characterize chemical elements. Besides the C signal from the TEM grid, Zn, O, and Si atoms were detected at the heterointerface between the ZnO film and the Si substrate. Because the EDX equipment detects x rays emitted by the matter in response to being hit with charged particles,[13] the EDX spectrum does not show other components such as molecules of SiO_2, ZnO, or $ZnSiO_3$.

a)Author to whom correspondence should be addressed. Electronic mail: twk@hanyang.ac.kr.

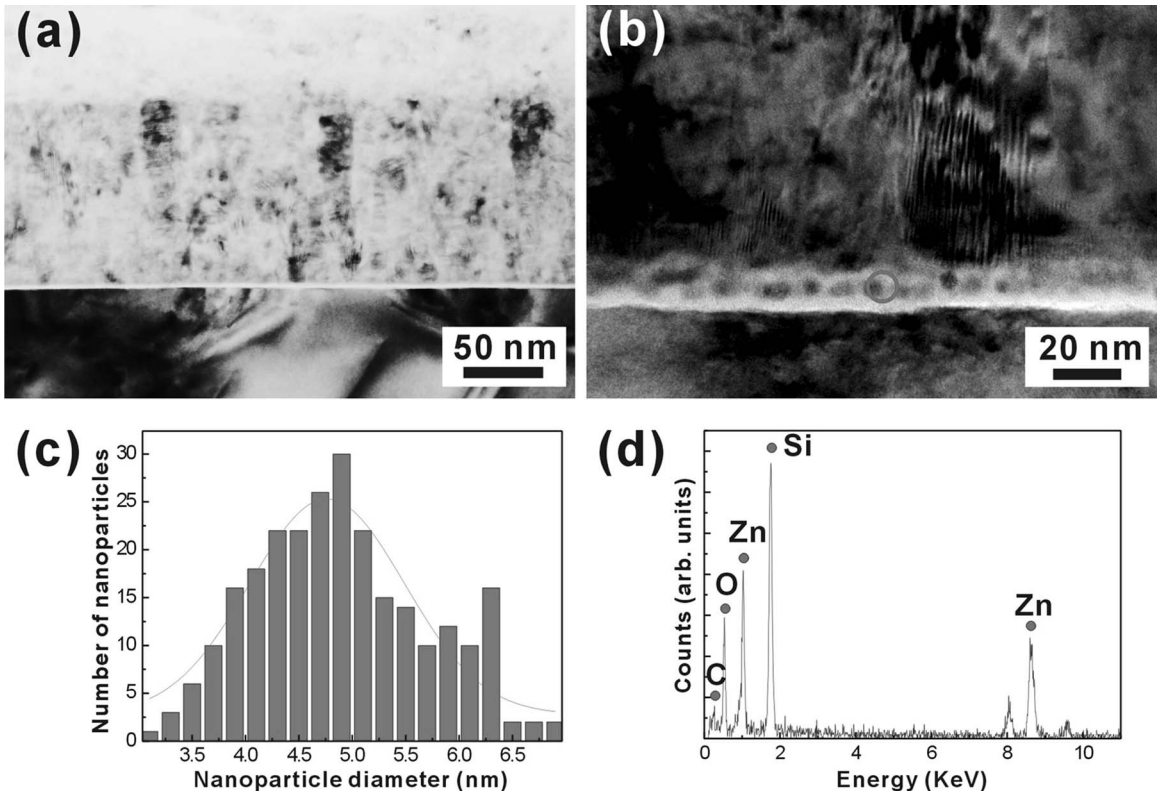

FIG. 1. (a) Cross-sectional bright-field TEM images of (a) an as-grown ZnO thin film grown on a *n*-Si (001) substrate and of (b) a ZnO thin film grown on a *n*-Si (001) substrate and annealed at 900 °C for 5 min. (c) The line represents a Gaussian fit to the nanocrystal diameter histogram. (d) EDX spectrum taken from the circled area in (b).

This result indicates that the formation of Zn nanocrystals originates from the diffusion of Si atoms from the Si substrate.[6]

Figures 2(a) and 2(b) show HRTEM images of the Zn nanocrystals with zone axes along the $[1\bar{2}1\bar{3}]$ and the [0001] directions and the corresponding FFT electron-diffraction patterns (insets). The well-defined crystallographic lattice spacings and angles of the Zn nanocrystals shown in the HRTEM images are in reasonable agreement with those of metallic zinc lattices, indicating that the Zn nanocrystals are single crystals.[6] The FFT electron-diffraction patterns show that the Zn nanocrystals embedded in the SiO_2 layer have a hexagonal structure.

Figure 3(a) shows a cross-sectional bright-field TEM image of the ZnO thin film grown on a *n*-Si (001) substrate annealed at 900 °C for 10 min. When the as-grown sample was annealed at 900 °C for 10 min, an amorphous SiO_2 layer with a thickness of approximately 20 nm was formed between the ZnO thin film and the Si substrate, and two layers of monoclinic $ZnSiO_3$ nanocrystals with an average diameter of 5 nm were formed in the dielectric SiO_2 layer, as shown in Fig. 3(b). Figure 3(c) shows the EDX spectrum, taken from the circled area denoted in Fig. 3(a), used to identify and characterize chemical elements. Besides the C signal from the TEM grid, Zn, O, and Si atoms were detected at the heterointerface between the ZnO film and the Si substrate. However, the Zn/Si ratio significantly increases with increasing annealing time, which is confirmed by Figs. 1(d)

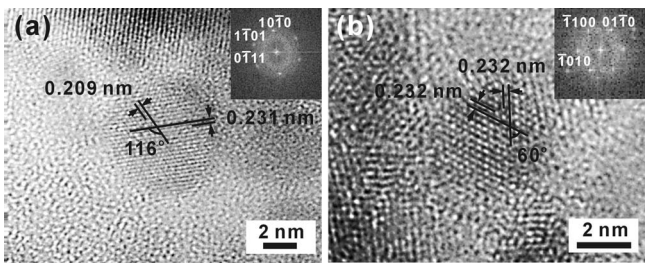

FIG. 2. HRTEM images of Zn nanocrystals with zone axes along (a) the $[1\bar{2}1\bar{3}]$ and (b) the [0001] directions and the corresponding FFT electron-diffraction patterns (insets).

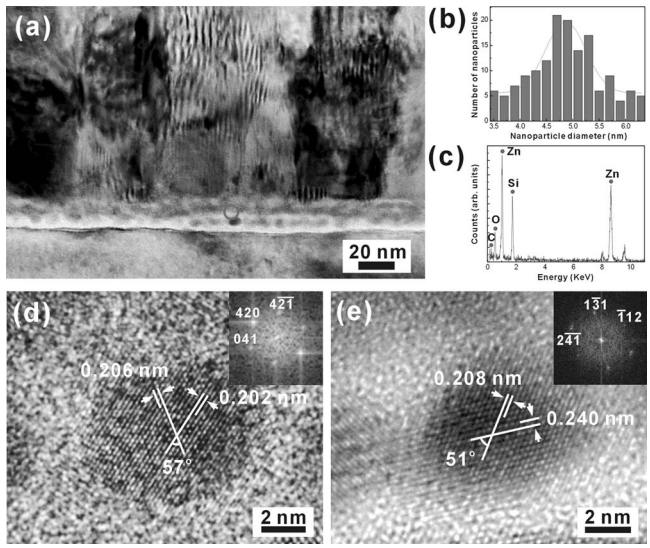

FIG. 3. (a) Cross-sectional bright-field TEM image of the sample annealed at 900 °C for 10 min. (b) The line represents a Gaussian fit to the nanocrystal diameter histogram. (c) EDX spectrum taken from the circled area in (a). HRTEM images of monoclinic $ZnSiO_3$ nanocrystals with zone axes along (d) the $[1\bar{2}8]$ and (e) the [732] directions and the corresponding FFT electron-diffraction patterns (insets).

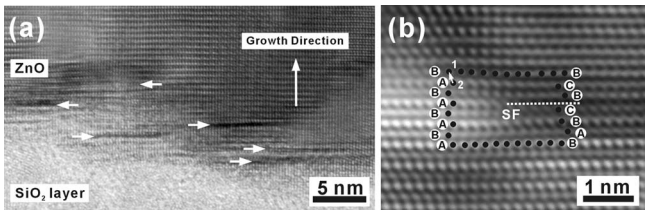

FIG. 4. HRTEM images indicating (a) stacking faults, shown by the arrows, at the interface and (b) a partial dislocation around a stacking fault in the ZnO film with a Burgers vector $\mathbf{b}=1/6\ \langle 02\bar{2}3\rangle$. A Burgers circuit with a starting point 1 and an end point 2 is displayed in (b).

and 3(c). The HRTEM images of Figs. 3(d) and 3(e) represent monoclinic $ZnSiO_3$ nanocrystals with zone axes along the $[1\bar{2}8]$ and the [732] directions and the corresponding FFT electron-diffraction patterns (insets). The lattice spacings and the angles of the HRTEM images shown in Figs. 3(d) and 3(e) are in reasonable agreement with those of $ZnSiO_3$ crystal lattices, indicating that the $ZnSiO_3$ nanocrystals are single crystals.[14] The corresponding FFT electron-diffraction patterns indicate that the $ZnSiO_3$ nanocrystals embedded in the SiO_2 layer have a monoclinic structure.

Figure 4(a) shows the HRTEM image along the $[2\bar{1}\bar{1}0]$ zone axis in the bottom region of the ZnO thin film annealed at 900 °C for 10 min. Many stacking faults, indicated by the arrows, exist around the heterointerface between the ZnO film and the amorphous SiO_2 layer along the (0002) planes. The Burgers circuit around the dislocation core is noted to determine the Burgers vector on the $(2\bar{1}\bar{1}0)$ plane projection of the partial dislocation, as shown in Fig. 4(b). The closed vector, which points from the end point [as denoted by the number 2 in Fig. 4(b)] to the starting point [as denoted by the number 1 in Fig. 4(b)] of the Burgers circuit, corresponds to the Burgers vector $\mathbf{b}=1/6\ \langle 02\bar{2}3\rangle$. The intrinsic type-I stacking fault is characterized by a stacking sequence AaBbAaBb|CcBbCc, where the capital and the small letters denote Zn or O atoms occupying a (0002) double layer, respectively.[15] The intrinsic type-I stacking fault results from the generation of Zn vacancy layers.[15]

The subsequent processes of deposition and thermal annealing contribute to the formation of Zn and $ZnSiO_3$ nanocrystals. The formation mechanisms for metallic Zn nanocrystals and the mechanisms for transforming from Zn nanocrystals to $ZnSiO_3$ nanocrystals can be suggested on the basis of the experimental results. The free energy for the formation of the SiO_2 layer at ~900 °C ($\Delta G_f = \sim -165$ kcal/mol) is much larger than that of the ZnO layer ($\Delta G_f = \sim -106$ kcal/mol).[16,17] Furthermore, the deposited or reacted thin films of ZnO or SiO_2 do not always contain stoichiometric oxygen content. This results in the occurrence of substoichiometric oxide layers. Although the ZnO is chemically very stable at room temperature, the suboxide SiO_x prefers to take oxygen away from ZnO_x and to be oxidized into the thermodynamically more stable SiO_2 at 900 °C, resulting in a transformation of the ZnO_x layer into a metallic Zn layer. When the ZnO/Si heterostructure is annealed at 900 °C for 10 min, the locally concentrated Zn region interrupts the formation of the amorphous SiO_2 structure due to the diffusion of Zn atoms into the amorphous SiO_2 layer, resulting in the formation of monoclinic $ZnSiO_3$ nanocrystals with a stable stoichiometry in the interface. This behavior is in reasonable agreement with the results of a theoretical simulation.[18] Because monoclinic crystalline $ZnSiO_3$ is very stable over a broad range of temperatures and pressures,[14] the $ZnSiO_3$ nanocrystals become stabilized due to the transformation from Zn nanocrystals with increasing Zn atoms resulting from an increase in the annealing time.

In summary, the bright-field TEM images, the HRTEM images, the FFT electron-diffraction patterns, and the EDX spectra showed that metallic Zn nanocrystals and insulating $ZnSiO_3$ nanocrystals were formed and embedded in a SiO_2 layer by thermally annealing a ZnO thin film deposited on a *n*-Si (001) substrate. The formed Zn nanocrystals were transformed into two layers of monoclinic $ZnSiO_3$ nanocrystals with an average diameter of 5 nm, with the increasing number of Zn atoms resulting from an increase in the annealing time from 5 to 10 min. The mechanisms underlying the transformation from Zn nanocrystals to $ZnSiO_3$ nanocrystals in a SiO_2 matrix due to thermal treatment were described on the basis of the experimental results.

This work was supported by the Korea Science and Engineering Foundation (KOSEF) grant funded by the Korea government (MEST) (Grant No. R0A-2007-000-20044-0). The authors would like to thank Dr. Youn-Joong Kim at the Korea Basic Science Institute for the use of the high-voltage TEM.

[1] S. J. Baik and K. S. Lin, Appl. Phys. Lett. **81**, 5186 (2002).
[2] E. Kapetanakis, P. Normand, D. Tsoukalas, and K. Beltsios, Appl. Phys. Lett. **80**, 2794 (2002).
[3] M. Perego, S. Ferrari, M. Fanciulli, G. B. Assayag, C. Bonafos, M. Carrada, and A. Claverie, J. Appl. Phys. **95**, 257 (2004).
[4] M. Kanoun, A. Souifi, T. Baron, and F. Mazon, Appl. Phys. Lett. **84**, 5079 (2004).
[5] V. Ramaswamy, T. E. Haynes, C. W. White, W. J. MoberlyChan, S. Roorda, and M. J. Aziz, Nano Lett. **5**, 373 (2005).
[6] T. W. Kim, J. W. Shin, J. Y. Lee, J. H. Jung, J. W. Lee, W. K. Choi, and S. Jin, Appl. Phys. Lett. **90**, 051915 (2007).
[7] T. Komeda, Y. Kim, M. Kasai, B. N. J. Persson, and H. Ueba, Science **295**, 2055 (2002).
[8] J. Heitmann, F. Müller, M. Zacharias, and U. Gösele, Adv. Mater. (Weinheim, Ger.) **17**, 795 (2005).
[9] S. Ağan, A. Dana, and A. Aydmh, J. Phys.: Condens. Matter **18**, 10705 (2006).
[10] T. Sass, V. Zela, A. Gustafsson, I. Pietzonka, and W. Seifert, Appl. Phys. Lett. **81**, 3455 (2002).
[11] J. M. Yuk, J. Y. Lee, J. H. Jung, D. U. Lee, T. W. Kim, D. I. Son, and W. K. Choi, J. Appl. Phys. **103**, 083520 (2008).
[12] Y. S. Jung, O. Kononenko, J. S. Kim, and W. K. Choi, J. Cryst. Growth **274**, 418 (2005).
[13] J. Zhou, J. Liu, X. Wang, J. Song, R. Tummala, N. S. Xu, and Z. L. Wang, Small **3**, 622 (2007).
[14] N. Morimoto, Y. Nukajima, Y. Syono, S. Akimoto, and Y. Matsui, Acta Crystallogr., Sect. B: Struct. Crystallogr. Cryst. Chem. **31**, 1041 (1975).
[15] J. M. Yuk, J. Y. Lee, T. W. Kim, D. I. Son, and W. K. Choi, J. Mater. Res. **23**, 1082 (2008).
[16] C. H. P. Lupis, *Chemical Thermodynamics of Materials* (North-Holland, New York, 1983), Vol. 1, p. 134.
[17] B. Thomas, *Reed, Free Energy of Formation of Binary Compounds* (MIT, Cambridge, 1971), Vol. 1, pp. 7–9.
[18] A. B. Rosenthal and S. H. Garofalini, J. Non-Cryst. Solids **87**, 254 (1986).